Pathogens and Disease, 2022, **80**, 1–12
DOI: 10.1093/femspd/ftac007
Advance access publication date: 7 April 2022
Research Article

Expression and structure of the *Chlamydia trachomatis* DksA ortholog

Cameron Mandel[1], Hong Yang[1], Garry W. Buchko[2,3,4], Jan Abendroth[4,5], Nicole Grieshaber[6], Travis Chiarelli[6], Scott Grieshaber[6], Anders Omsland[1,*]

[1]Paul G. Allen School for Global Health, Washington State University, Pullman, WA 99164, USA
[2]School of Molecular Biosciences, Washington State University, Pullman, WA 99164, USA
[3]Earth and Biological Sciences Directorate, Pacific Northwest National Laboratory, Richland, WA 99354, USA
[4]Seattle Structural Genomics Center for Infectious Disease, WA, USA
[5]UCB, Bainbridge Island, WA 98110, USA
[6]Department of Biological Sciences, University of Idaho, Moscow, ID 83844, USA
***Corresponding author:** Paul G. Allen School for Global Health, Washington State University, Pullman, WA 99164, USA. Tel: +1-509-335-3916; E-mail: anders.omsland@wsu.edu
One sentence summary: Expression of the protein DksA in *Chlamydia trachomatis* is regulated with the bacterium's developmental cycle. Ectopic expression of DksA affects generation of infectious bacterial progeny.
Editor: Guangming Zhong

Abstract

Chlamydia trachomatis is a bacterial obligate intracellular parasite and a significant cause of human disease, including sexually transmitted infections and trachoma. The bacterial RNA polymerase-binding protein DksA is a transcription factor integral to the multicomponent bacterial stress response pathway known as the stringent response. The genome of *C. trachomatis* encodes a DksA ortholog ($DksA_{Ct}$) that is maximally expressed at 15–20 h post infection, a time frame correlating with the onset of transition between the replicative reticulate body (RB) and infectious elementary body (EB) forms of the pathogen. Ectopic overexpression of $DksA_{Ct}$ in *C. trachomatis* prior to RB–EB transitions during infection of HeLa cells resulted in a 39.3% reduction in overall replication (yield) and a 49.6% reduction in recovered EBs. While the overall domain organization of $DksA_{Ct}$ is similar to the DksA ortholog of *Escherichia coli* ($DksA_{Ec}$), $DksA_{Ct}$ did not functionally complement $DksA_{Ec}$. Transcription of $dksA_{Ct}$ is regulated by tandem promoters, one of which also controls expression of *nrdR*, encoding a negative regulator of deoxyribonucleotide biosynthesis. The phenotype resulting from ectopic expression of $DksA_{Ct}$ and the correlation between $dksA_{Ct}$ and *nrdR* expression is consistent with a role for $DksA_{Ct}$ in the *C. trachomatis* developmental cycle.

Keywords: *Chlamydia*, transcription, riboswitch, morphological transition

Introduction

Chlamydia trachomatis is a human-adapted bacterial obligate intracellular parasite and different pathotypes (aka serovars) of the pathogen cause distinct diseases. Urogenital serovars of *C. trachomatis* are a major cause of sexually transmitted infections (Stamm 1999, Rowley *et al.* 2012), while ocular serovars can cause trachoma (Burton and Mabey 2009), a leading cause of preventable blindness most prevalent in developing areas with poor sanitation. During infection of cultured host cells, *C. trachomatis* transitions between two physiologically distinct cell forms: the infectious but non-replicative elementary body (EB) and the replicative but noninfectious reticulate body (RB) (Shaw *et al.* 2000). While transition between cell forms is critical for replication and generation of infectious progeny, little is known about the trigger(s) or regulatory mechanism(s) that influence and control chlamydial morphological differentiation. Temporally restricted expression of different classes of genes during the chlamydial developmental cycle (Shaw *et al.* 2000, Belland *et al.* 2003) and recent genetic analysis identifying several genes with apparent functions in chlamydial development (Brothwell *et al.* 2016) suggest that EB–RB–EB transitions can occur in response to various stimuli and that response mechanisms controlling chlamydial development are redundant.

Chlamydia trachomatis has undergone genome reduction at the expense of reduced metabolic capacity (Stephens 1998). As a result, numerous essential nutrients are scavenged from the host cell during infection to allow for pathogen replication. In addition to biosynthetic deficiencies, certain regulatory pathways appear reduced to a single component of the canonical machinery. Consequently, *C. trachomatis* may have evolved to use these single components or 'orphan regulators' in place of certain canonical regulatory cascades.

In several bacteria, including *Escherichia coli* (Magnusson *et al.* 2007, Vinella *et al.* 2012, Kessler *et al.* 2017), *Pseudomonas aeruginosa* (Perron *et al.* 2005) and *Legionella pneumophila* (Dalebroux *et al.* 2010), DksA is a relatively small (<160 residue) RNA polymerase (RNAP)-binding protein and global transcriptional regulator that integrates responses to diverse stimuli, including nutrient availability (Paul *et al.* 2005), via a multicomponent response mechanism referred to as the stringent response (Cashel and Gallant 1969, Cashel *et al.* 1996, Potrykus and Cashel 2008, Traxler *et al.* 2008). The *C. trachomatis* genome encodes a DksA ortholog,

Received: November 16, 2021. **Revised:** February 15, 2022. **Accepted:** April 4, 2022

CTL0664 ($DksA_{Ct}$). The signaling nucleotide guanosine tetraphosphate (ppGpp) can be produced in response to nutrient (e.g. amino acid) starvation and functions with other regulatory components of the stringent response, including DksA (Magnusson *et al.* 2005, 2007, Ferullo and Lovett 2008, Traxler *et al.* 2008, Geiger *et al.* 2010). *Chlamydia trachomatis* does not encode any apparent ortholog for proteins involved with ppGpp biosynthesis or breakdown (Mittenhuber 2001, Hauryliuk *et al.* 2015), and attempts to detect ppGpp in *C. trachomatis* have been unsuccessful (data not shown). The ability of DksA to function independently of ppGpp in *E. coli* and *Rhodobacter sphaeroides* (Magnusson *et al.* 2007, Vinella *et al.* 2012, Lennon *et al.* 2014) demonstrates that DksA is capable of functioning as an independent regulator. Additionally, in the biphasic developmental cycle of *L. pneumophila*, DksA has been shown to govern bacterial differentiation from the replicative form to the virulent form in cooperation with ppGpp (Dalebroux *et al.* 2010). We hypothesize that $dksA_{Ct}$ is maintained as a gene associated with RB–EB transitions in the chlamydial developmental cycle.

To probe the role of $dksA_{Ct}$ in chlamydial biology, we determined the expression of $DksA_{Ct}$ during the chlamydial developmental cycle and tested the effect of $DksA_{Ct}$ expression on *C. trachomatis* replication and EB generation following ectopic expression of $dksA_{Ct}$. Additionally, we resolved the 3D structure of $DksA_{Ct}$, assessed the ability of $DksA_{Ct}$ to functionally complement $DksA_{Ec}$ and identified promoter sites for $dksA_{Ct}$.

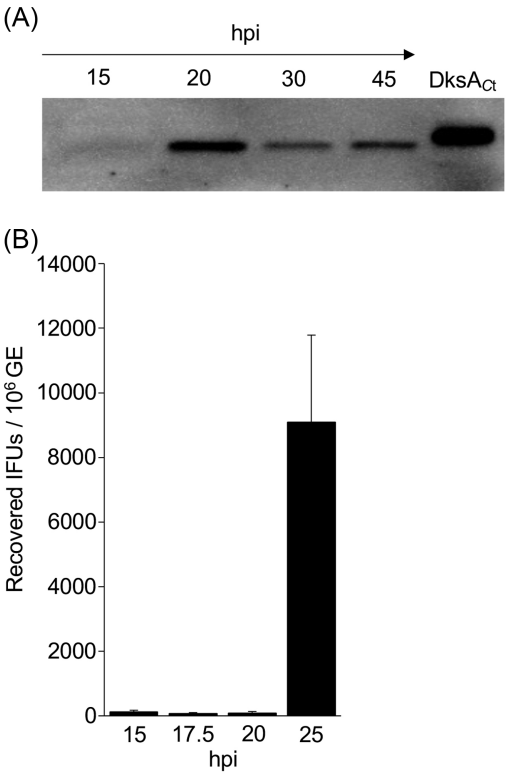

Figure 1. $DksA_{Ct}$ expression is maximal in RBs and coincides with initiation of RB–EB transition. To determine whether $DksA_{Ct}$ expression is temporally regulated, expression of the native protein was determined at critical stages of the developmental cycle. **(A)** Western blot of *C. trachomatis* whole-cell lysates normalized to GE. Time points were chosen to include cell populations that were predominantly RBs (15 hpi, 20 hpi), mixed RBs and EBs (30 hpi), and predominantly EBs (45 hpi) ($n = 2$). **(B)** IFU assay depicting the relative abundance of infectious EBs at different time points of the chlamydial developmental cycle ($n = 3$).

Results and discussion

Native expression of $DksA_{Ct}$ is maximal at the intermediate-late stages of the chlamydial developmental cycle

During infection of HeLa cells, *C. trachomatis* L2 undergoes a predictable developmental cycle in which log phase RBs initiate transition to the EB form approximately 18 h post infection (hpi) (Grieshaber *et al.* 2018). To determine whether $DksA_{Ct}$ expression is temporally synchronized with RB–EB transitions, bacteria were isolated from infected HeLa cells at time points correlating with critical stages of the chlamydial developmental cycle and protein expression determined by western blot using a $DksA_{Ct}$-specific antibody (Fig. 1A). $DksA_{Ct}$ expression was normalized to the number of bacteria by measuring genome equivalents (GE) (Skipp *et al.* 2016). While minimal (if any) $DksA_{Ct}$ was detected in bacteria recovered at 15 hpi, a time point correlating with replicating RBs, maximal expression was observed at 20 hpi, a time point in the developmental cycle coincident with initiation of RB to EB morphological transitions. A similar expression pattern was previously reported for DksA in *C. pneumoniae* (Mukhopadhyay *et al.* 2006), indicating that DksA expression profiles are conserved between pathogenic *Chlamydia* species. $DksA_{Ct}$ was detected at moderately reduced levels at 30 and 45 hpi. Western blot analysis of EBs purified by density gradient centrifugation after sonication confirmed expression of $DksA_{Ct}$ in this cell form (data not shown). The dynamic expression pattern of $DksA_{Ct}$ is unique compared with the stable expression observed for $DksA_{Ec}$ (Paul *et al.* 2004, Brown *et al.* 2002). Because the RB form contains more protein per cell than the EB, the method of normalization will influence the measured level of expression of any protein in *C. trachomatis*. The RB contains ~10-fold more protein compared with the EB on a per cell basis (Omsland *et al.* 2012), indicating $DksA_{Ct}$ levels remain high in the EB form. To determine the relative population of infectious EBs in infected HeLa cultures, inclusion forming unit (IFU) assays were performed (Fig. 1B). Few detected inclusions following infection with bacteria harvested at 15–20 hpi indicate that initiation of $DksA_{Ct}$ expression occurs at a time point when the intracellular chlamydial population predominantly consists of replicating RBs. Development of inclusions in cultures infected with bacteria recovered at 25 hpi was used as a positive control for the assay.

Overexpression of $DksA_{Ct}$ prior to RB–EB transition reduces both replication and production of infectious progeny

To test whether early expression of $dksA_{Ct}$ affects replication and/or production of infectious EBs, *C. trachomatis* was transformed with the inducible riboswitch construct pBOMB4::E-Riboswitch-$dksA_{Ct}$ (R-$dksA_{Ct}$). Additionally, to ensure any phenotype observed upon induction of the R-$dksA_{Ct}$ construct is not a nonspecific effect of protein expression, HeLa cultures were infected with *C. trachomatis* transformed with p2TK2-SW2::E-Riboswitch-Clover (R-Clover) (Grieshaber *et al*, 2022) and expression of Clover, a variant for green fluorescent protein, used as a control. Replication was measured via analysis of GE in samples harvested at 30 hpi in the absence or presence of 0.5 mM theophylline, added at the time of infection. Induced expression of $DksA_{Ct}$ resulted in a 39.3% reduction in GE compared with non-induced control cultures (Fig. 2A). No significant effect on replication was observed with ectopic expression of Clover. These data suggest that the negative impact of early expression of $DksA_{Ct}$ on

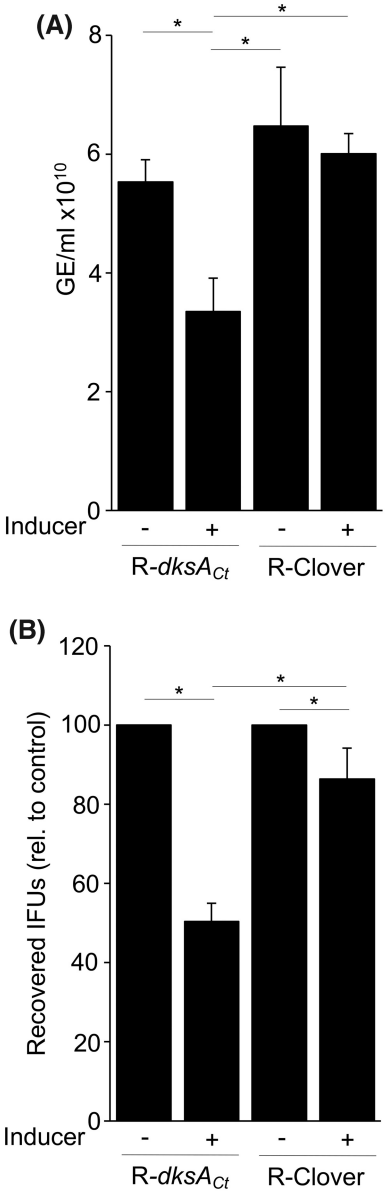

Figure 2. Ectopic expression of $DksA_{Ct}$ results in reduction in *C. trachomatis* intracellular replication and recovered IFUs. The effect of $DksA_{Ct}$ expression on *C. trachomatis* growth and EB generation was tested by theophylline-induced ectopic expression during infection of HeLa cells. **(A)** Infection of HeLa cells with R-$dksA_{Ct}$ in the presence of theophylline resulted in a 39.3% ($P = 0.0115$, $n = 3$) reduction in GE when compared with the non-induced R-$dksA_{Ct}$ control, and 48.2% ($P = 0.0012$, $n = 3$) and 44.1% ($P = 0.0036$, $n = 3$) reduction in GE when compared with non-induced or induced R-Clover, respectively. Induction of R-Clover expression did not significantly affect measured GE ($P = 0.7931$, $n = 3$) when compared with non-induced control. **(B)** IFU assays conducted with samples normalized to GE showed a 49.6% ($P < 0.0001$, $n = 3$) and 13.6% ($P = 0.0428$, $n = 3$) reduction in recovered IFUs for induced R-$dksA_{Ct}$ and R-Clover, respectively, when compared with non-induced controls (set to 100%). The number of recovered IFUs following induction of R-$dksA_{Ct}$ was 36% less than that observed with induced R-Clover ($P = 0.0004$, $n = 3$). P-values were calculated using one-way analysis of variance (ANOVA) with Tukey's post hoc test.

replication is specific to $DksA_{Ct}$ activity and is not due to nonspecific effects of induced protein expression.

To assess whether early expression of $dksA_{Ct}$ similarly impacts the chlamydial developmental cycle, generation of infectious progeny was measured by performing IFU assays with inocula normalized to GE. Induction of R-$dksA_{Ct}$ resulted in a 49.6% reduction in recovered IFUs as compared with non-treated control cultures (Fig. 2B). Relative EB abundance quantified via an IFU assay for bacteria transformed with R-Clover resulted in a 13.6% reduction in recovered IFUs in the presence of inducer (Fig. 2B). To determine whether the reduction in IFUs observed following induction of R-Clover was related to the protein and/or use of theophylline, the effect of theophylline on wild-type *C. trachomatis* L2 was determined. Although wild-type bacteria showed statistically significant differences in both replication and recovered IFUs in response to theophylline (Fig. S1, Supporting Information), the effect was less than that observed for bacteria transformed with R-$dksA_{Ct}$, consistent with an effect of $DksA_{Ct}$ in chlamydial replication and development (GE: 18% vs 39.3%; IFU: 17.7% vs 49.6%). Compared with induction of R-Clover, induction of R-$dksA_{Ct}$ resulted in a statistically significant 36% reduction in recovered IFUs (Fig. 2B). Successful induction of R-$dksA_{Ct}$ and R-Clover by theophylline was confirmed via western blot or fluorescence microscopy, respectively (Fig. S2, Supporting Information).

$DksA_{Ct}$ retains major structural characteristics of DksA proteins

Amino acid sequence identity is commonly used as an indicator for predicting conservation of protein function (Tian and Skolnick 2003, Capra and Singh 2007, Krissinel 2007). Amino acid sequence alignment of DksA from various chlamydial species and multiple orthologs for which the crystal structures have been determined ($DksA_{Ec}$, $DksA_{Pa}$ and $DksA_{Af}$) indicated high sequence conservation within the *Chlamydia* genus, and low sequence identity between the *Chlamydia* proteins and those encoded by genes in other bacteria (Fig. 3). Among human-adapted *Chlamydia* species, $dksA_{Ct}$ showed the highest identity with *C. pneumoniae* (90% identity at the amino acid level). In addition to apparent high conservation across the *Chlamydia* genus, homologs of *dksA* can also be found in nonpathogenic *Protochlamydia amoebophila* UWE25 and *Protochlamydia naegleriophila* KNic (Clark *et al.* 2016). Despite low (~10%) primary sequence identity (Perederina *et al.* 2004, Rutherford *et al.* 2007), the transcription elongation factor GreA ($GreA_{Ec}$) has been shown to assume the physiological function of DksA in *E. coli* Δ*dksA* $ppGpp^0$ mutants (Vinella *et al.* 2012), indicating that sequence identity does not consistently correlate with conserved function in this family of transcription factors.

Sequence analyses of DksA proteins from several bacteria has shown that while extensive diversity exists in the primary amino acid sequences, all proteins contain a conserved four-cysteine (C4) zinc-finger motif, CxxC-(x17)-CxxC, or a two-cysteine (C2) or one-cysteine (C1) zinc-independent motif, CxxS/T-(x17)-C/S/TxxA, with the first cysteine always conserved (Perederina *et al.* 2004, Henard *et al.* 2014). While the C4 proteins are sometimes referred to as DksA and the C2 and C1 proteins as DksA2 (Furman *et al.* 2013), here we will refer to all three groups as DksA proteins. The genomes of *Chlamydia* species all contain a single less frequently observed C1-DksA ortholog. Structures have been determined for two C4-DksA proteins, *Escherichia coli* ($DksA_{Ec}$) (Perederina *et al.* 2004) and *Agrobacterium fabrum* ($DksA_{Af}$), and one C2-DksA protein, *P. aeruginosa* ($DksA_{Pa}$) (Furman *et al.* 2013). Prototypical DksA proteins contain two domains that interact with RNAP: an N-terminal, two helix, coiled-coil domain that has been shown to interact with the secondary channel of RNAP (Molodtsov *et al.* 2018) and a C-terminal globular domain containing the Cx-motif plus a C-terminal α-helix that jointly interact with the β' rim helices outside the RNAP secondary channel (Perederina *et al.* 2004,

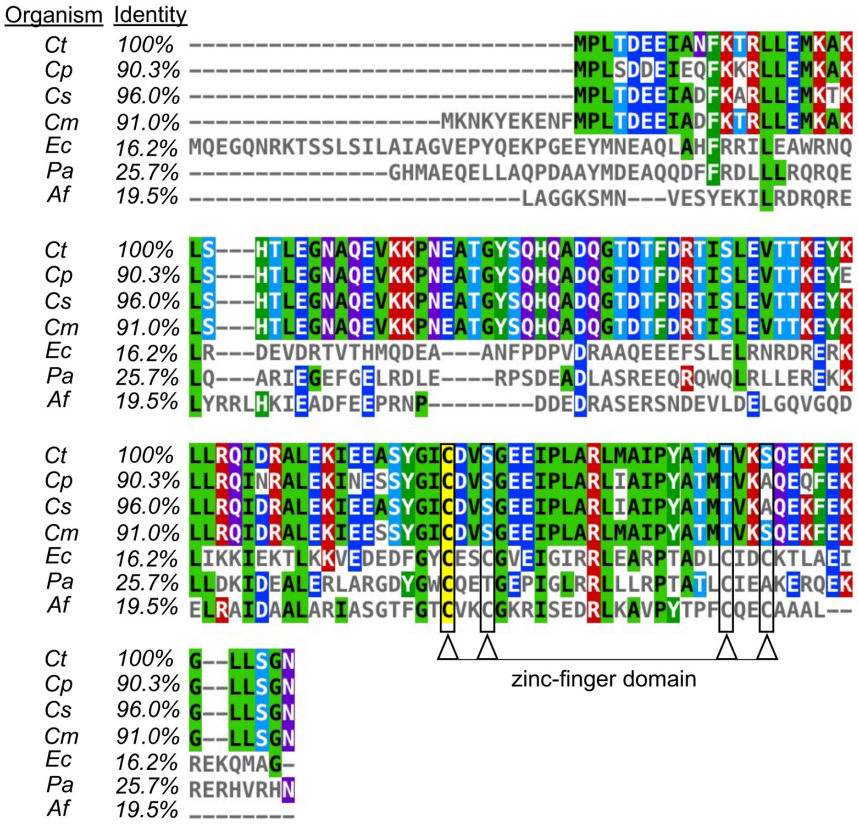

Figure 3. Primary sequence alignment of DksA proteins. Amino acid sequences of DksA proteins were assessed by comparing proteins with solved crystal structures and those of pathogenic chlamydiae. High sequence identity was observed for DksA between chlamydial species. *Ct* = *C. trachomatis*; *Cp* = *C. pneumoniae*; *Cs* = *C. suis*; *Cm* = *C. muridarum*; *Ec* = *E. coli*; *Pa* = *P. aeruginosa*; and *Af* = *A. fabrum*. The four-cysteine residues of the zinc-finger domain in the *E. coli* and *A. fabrum* proteins are indicated by arrowheads.

Lennon *et al.* 2012, Parshin *et al.* 2015). This interaction has high specificity, and it has been demonstrated in *E. coli* that a single point mutation in the C-terminal α-helix can result in loss of both binding and activity *in vitro* (Parshin *et al.* 2015). To facilitate a better general understanding of C1-DksA proteins and further elucidate the significance of widespread DksA conservation in *Chlamydia* (Domman and Horn 2015), we solved the 3D crystal structure of $DksA_{Ct}$.

Despite the relatively low resolution (2.95 Å) of the X-ray diffraction data, the final model had excellent refinement statistics (Table 1). Two protein molecules are observed in the asymmetric unit with the structure of each protomer having a backbone atom (N-C^{α}-C = O) root-mean-standard deviation of 0.33 Å between both chains (Fig. 4A). Superposition of the protein structures show that the topology of all four DksA protein structures are similar with four α-helices organized into two domains. The relative orientation of the two domains overlap in all four structures despite $DksA_{Pa}$ and $DksA_{Ct}$ containing two or one cysteine, respectively, and no zinc ion, further establishing that zinc is not required for function of DksA proteins (Furman *et al.* 2013). Instead, the cysteine and zinc content of DksA may impact its capacity to respond to reactive oxygen and nitrogen species (Henard *et al.* 2014, Crawford *et al.* 2016). Because all pathogenic chlamydiae appear to express a highly homologous C1-form of DksA, the protein may have evolved in these pathogens to maintain a functional structure in (intracellular) environments where zinc is not abundant. What is different between the four structures is the region towards the turn between α1 and α2 in the coiled coil domain. In the crystal structure of $DksA_{Ct}$ (C1-DksA), electron density is missing (E27-V62) and in the Nuclear Magnetic Resonance (NMR) structures for $DksA_{Af}$ (C4-DksA) there is no convergence of the calculated structures (K29-L58). These observations in crystal (Oldfield *et al.* 2013) and NMR (Konrat 2014) structures may be correlated to intrinsically disordered regions. On the other hand, the loop between α1 and α2 is significantly smaller for $DksA_{Pa}$ (chain C, R50-A58) and $DksA_{Ec}$ (F69-P70), averaging eight and two residues, respectively. To explore the possibility that this difference could be attributed to varying degrees of intrinsic disorder we analyzed all four primary amino acid sequences of the proteins depicted in Fig. 4A using IUPred2A (Mészáros *et al.* 2018, Erdős and Dosztányi 2020). Alignment of these sequences starting with the first residue of the first N-terminal α-helix identifies a region of ~20 residues between the first two N-terminal α-helices with IUPred scores above 0.5, the threshold for disorder, for three of the four proteins (~10 residues for $DksA_{Pa}$ showed scores below the cutoff) (Fig. S3, Supporting Information). We speculate that in monomeric DksA proteins the tip of the coiled coil domain is disordered with the helical regions at the C-terminal and N-terminal ends of α1 and α2, respectively, being transient in nature. This structural fluidity may be necessary for this domain to dock with the secondary channel of RNAP (Garner *et al.* 1999). These regions are more helical in the crystal structures of $DksA_{Pa}$ and $DksA_{Ec}$ perhaps only due to crystal packing contacts that restrict motion and stabilize the helical state (Oldfield *et al.* 2013).

Figure 4B is a cartoon representation of one of the two structures in the asymmetric unit showing that the protein contains

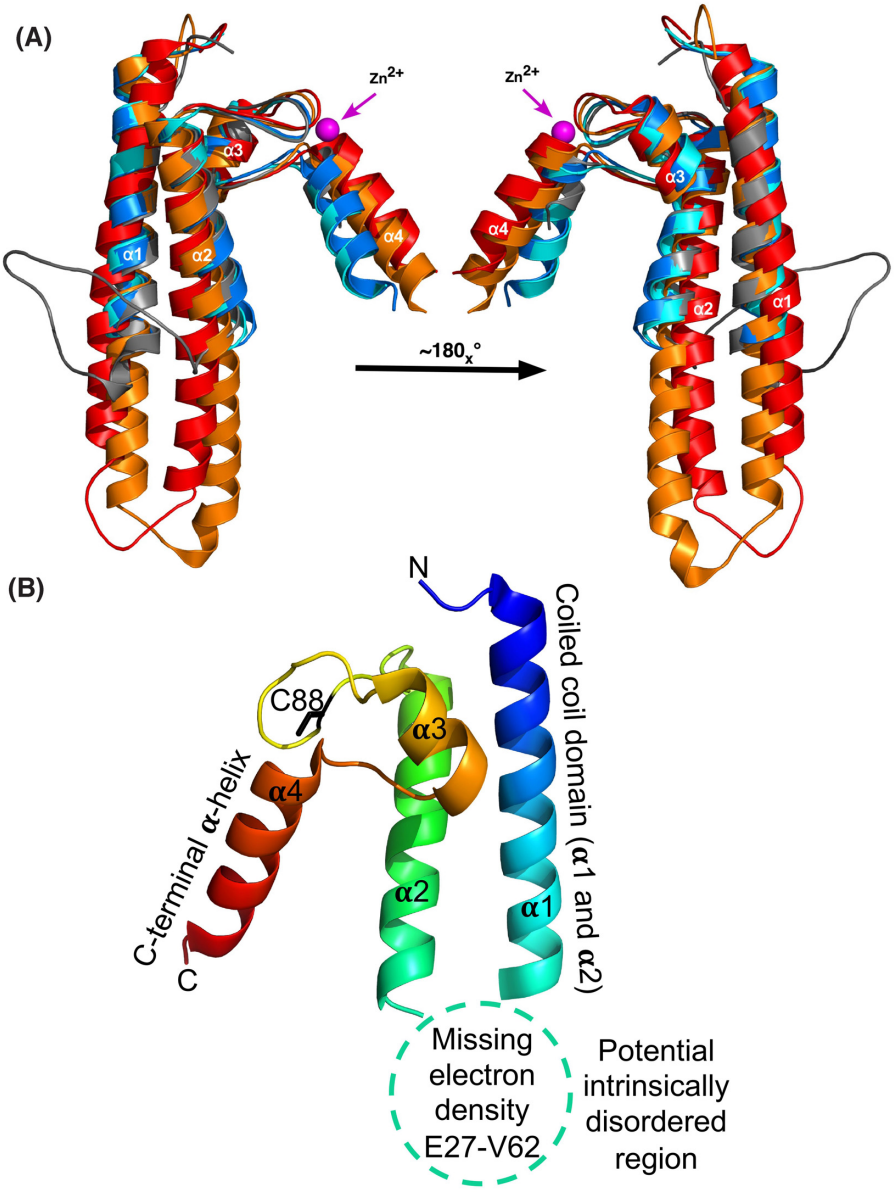

Figure 4. Structure of $DksA_{Ct}$. The 3D structure of $DksA_{Ct}$ was derived by X-ray diffraction. **(A)** Superposition of cartoon representations of both molecules in the asymmetric unit of $DksA_{Ct}$ (6PTG-B, marine and cyan, C1-DksA) with the crystal structure of $DksA_{Pa}$ (4IJJ-C, red, C2-DksA), $DksA_{Ec}$ (1TJL-F, orange, C4-DksA) and the NMR solution structure of $DksA_{Af}$ (2KQ9-Model_1, gray, C4-DksA) using the PDBeFold server (https://www.ebi.ac.uk/msd-srv/ssm/). The zinc ion in $DksA_{Af}$ is shown (magenta). **(B)** The overall domain structure of $DksA_{Ct}$ is consistent with that of other proteins known to bind the minor groove of RNA polymerase.

four α-helices with the N-terminal two helices forming a coiled coil domain and the two C-terminal helices part of a C-terminal globular domain containing a C1-motif. In both chains, electron density was insufficient to model the eight residues of the N-terminal tag, one or two residues at the C-terminus, and the region between L26(A)/E27(B) and V62, residues between the two helices of the coiled coil domain. No electron density corresponding to zinc or any other metal was observed.

$DksA_{Ct}$ does not functionally complement $DksA_{Ec}$

Complementation of *dksA*-deficient *E. coli* has been conducted successfully with genes encoding C4-, C2- and C1-DksA proteins (Blaby-Haas *et al.* 2011, Pal *et al.* 2012, Lennon *et al.* 2014). For example, the C1-DksA ortholog of the α-proteobacterium *R. sphaeroides* shares 42% identity with $DksA_{Ec}$, and has been shown to function alone and synergistically with ppGpp (Lennon *et al.* 2014). Divergent primary sequences, unresolved structural domains and the unique biology of *C. trachomatis* prompted analysis to determine whether $dksA_{Ct}$ can functionally complement the prototypical *E. coli* ortholog $dksA_{Ec}$. DksA functionality can be tested based on the role of DksA in regulating amino acid synthesis in *E. coli* during growth on minimal M9 medium (Jude *et al.* 2003). *dksA* complementation in *E. coli* has shown that the *dksA* genes of *Vibrio cholera* (Pal *et al.* 2012), *R. sphaeroides* (Lennon *et al.* 2014) and *P. aeruginosa* (Blaby-Haas *et al.* 2011) can functionally complement $dksA_{Ec}$. In our hands, *P. aeruginosa dksA* ($dksA1_{Pa}$) resulted in partial rescue of an *E. coli* mutant unable to express $dksA_{Ec}$, while complementation with $dksA_{Ct}$ did not restore the growth defect (Fig. 5). Moreover, complementation with *P. aeruginosa dksA2* ($dksA2_{Pa}$) did not result in recovery of the growth defect exhibited by *E. coli* lacking

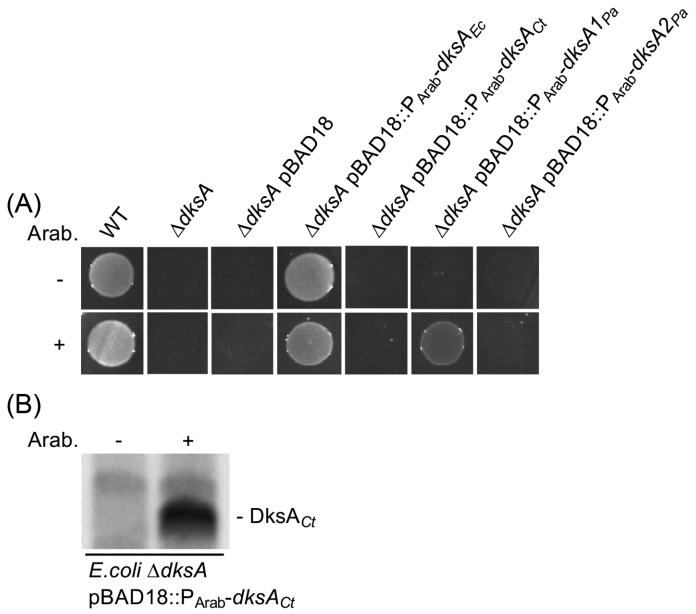

Figure 5. $dksA_{Ct}$ cannot functionally complement $dksA_{Ec}$. To test whether $dksA_{Ct}$ could functionally complement the *dksA* gene of the model organism *E. coli*, $dksA_{Ct}$ was used to complement a $dksA_{Ec}$ deletion mutant. **(A)** Complementation of *E. coli* Δ*dksA* with $dksA_{Ct}$, $dksA1_{Pa}$ or $dksA2_{Pa}$ plated on minimal medium. Complementation with $dksA_{Ec}$ or an empty vector were used as controls. **(B)** Arabinose induction of pBAD18::$dksA_{Ct}$ was confirmed via western blotting of strains following growth in Luria-Bertani (LB) broth.

Table 1. X-ray diffraction data for $DksA_{Ct}$.

Parameter	
PDB ID	6PTG
Space group	$P3_221$
Diffraction data	
a (Å)	83.42
b (Å)	83.42
c (Å)	99.03
$\alpha = \beta, \gamma$ (°)	90, 120
Matthews coefficient ($Å^3Da^{-1}$)	3.32
Solvent content (%)	63%
Resolution range (Å)	50–2.95 (3.03–2.95)
Mean $I/\sigma(I)$	20.54 (3.12)
No. of observed unique reflections	8668 (628)
Completeness (%)	98.8 (98.9)
Multiplicity	6.1 (6.2)
$R_{merge}{}^2$	0.068 (0.625)
CC 1/2	0.999 (0.890)
Refinement	
Resolution	50–2.95 (3.13–2.95)
No. of used reflections	8651 (1271)
R_{work}	0.1823 (0.2636)
R_{free}	0.2264 (0.3279)
RMSD bonds (Å)	0.004
RMSD angles (°)	0.54
Mean B factor overall ($Å^2$)	73.8
Mean B factor protein ($Å^2$)	74.1
MolProbity model analysis	
Clash score, all atoms	2.77
Ramachandran favored (%)	100
Ramachandran outliers (%)	0
Rotamer favored (%)	100
Rotamer outliers (%)	0
MolProbity score	1.07

the *dksA* gene. Growth in the absence of inducer is likely a result of leaky expression of $DksA_{Ec}$ in the *dksA* deletion mutant. Overall, $dksA_{Ct}$ does not have activity complementary to that of $dksA_{Ec}$ or $dksA1_{Pa}$ suggesting an alternative binding motif or function for $dksA_{Ct}$ compared with that of prototypical DksA proteins.

$dksA_{Ct}$ expression is regulated from promoter sites both upstream of and within *nrdR*

Gene linkage and co-expression can be related to the function of two or more genes in a coordinated biological process. In all chlamydial genomes analyzed, *dksA* is located immediately downstream of *nrdR*, encoding the NrdA/B repressor NrdR, a negative regulator of deoxyribonucleotide synthesis. *lspA*, encoding a lipoprotein signal peptidase, is located immediately downstream of $dksA_{Ct}$. The genomic localization and organization of *dksA* with *nrdR* and *lspA* in chlamydial genomes, and intergenic regions of only 5–24 bp, are consistent with their control by a single promoter upstream of *nrdR*. This conserved orientation provides a potential link between the role of *dksA* and the metabolic function of *nrdR* in nucleic acid metabolism. Previously published deep sequencing data indicate that *nrdR*, *dksA* and *lspA* in *C. pneumoniae* are transcribed as a polycistronic mRNA (Albrecht *et al.* 2011) and suggest that the same may be true in *C. trachomatis* (Albrecht *et al.* 2010).

To determine whether $dksA_{Ct}$ could be regulated from an independent promoter downstream of the promoter controlling expression of the *nrdR*-$dksA_{Ct}$-*lspA* operon, *C. trachomatis* was transformed with transcriptional reporter constructs based on the pBOMB vector (Bauler and Hackstadt 2014) containing sequences 830 or 469 bp upstream of $dksA_{Ct}$ linked to GFP-LVA (Fig. 6A). Constitutive expression of mCherry was used as a positive control for transformation. GFP was detected regardless of construct configuration suggesting that $dksA_{Ct}$ can be transcribed from promoters both upstream of and within *nrdR* (Fig. 6B). No signal was detected from the empty vector control.

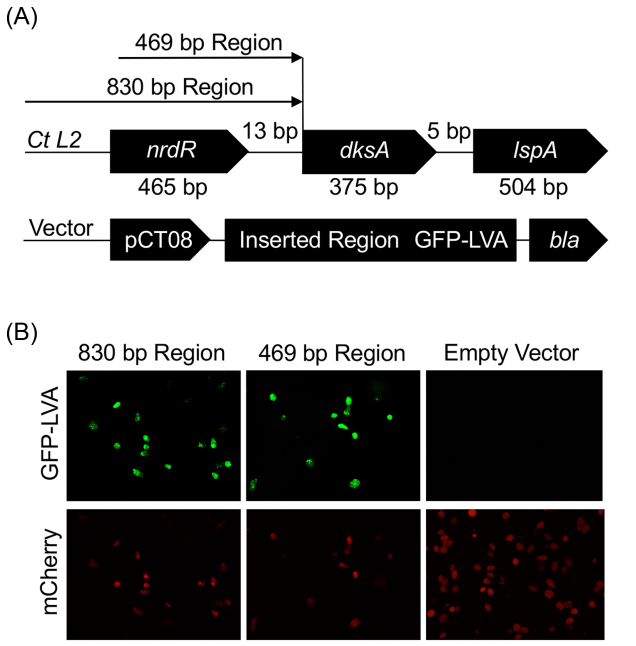

Figure 6. Expression of $dksA_{Ct}$ is controlled by two promoters. The possibility that $dksA_{Ct}$ expression can be controlled independently of *nrdR* was tested using a transcriptional reporter construct. **(A)** Schematic representation of the *C. trachomatis* genome with sequences upstream of $dksA_{Ct}$ containing potential promoters, and the reporter construct used to test expression. **(B)** Fluorescence micrographs (×200 magnification, 45 hpi) reveal expression of GFP-LVA regardless of promoter region used. Constitutive mCherry expression was used to confirm transformation. No signal from GFP-LVA was observed in the empty vector control. Equivalent reporter expression was observed in both mixed populations of transformants under antibiotic selection ($n = 3$) and in clonally isolated transformants ($n = 1$).

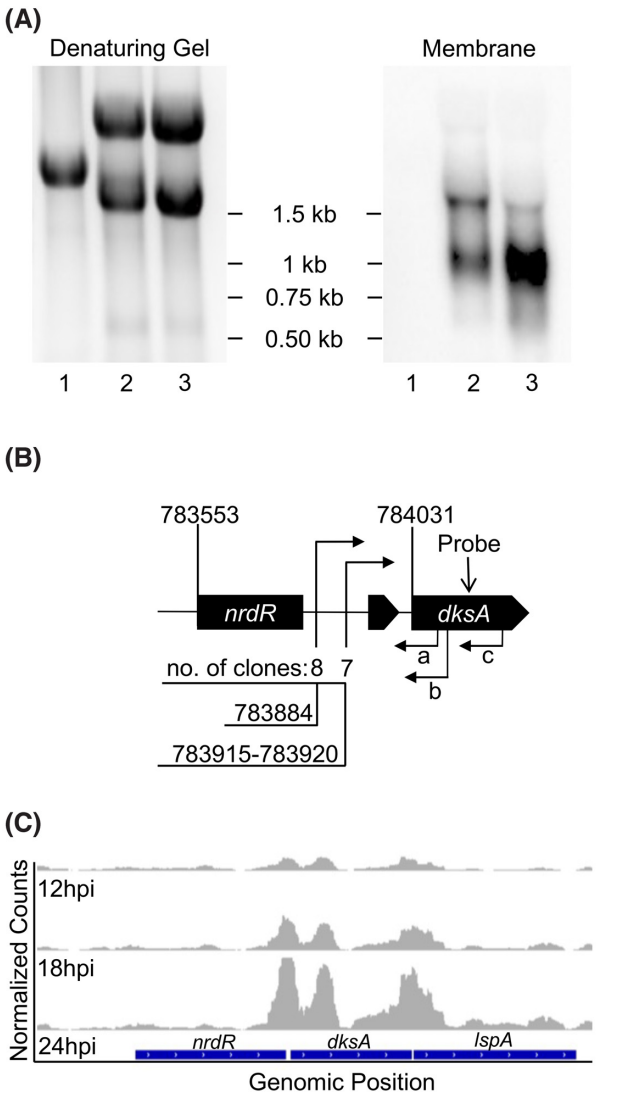

Figure 7. $dksA_{Ct}$ is expressed as two distinct transcripts. Northern blot analysis was used to confirm expression of $dksA_{Ct}$ as two distinct RNA species. **(A)** Denaturing gel stained with EtBr and corresponding membrane hybridized with a biotinylated probe complementary to a segment of $dksA_{Ct}$ visualized using chemiluminescence. Total RNA extracted from noninfected HeLa cells was used as a control for nonspecific binding of the probe to host RNA. Lane 1: RNA from uninfected HeLa cells. Lane 2: RNA isolated from *C. trachomatis*-infected HeLa cells, 20 hpi ($n = 2$). Lane 3: RNA isolated from *C. trachomatis*-infected HeLa cells, 30 hpi ($n = 3$). All lanes were loaded with 15 μg RNA. **(B)** Schematic showing the relative locations for $dksA_{Ct}$-specific primers (a, b and c) used to determine the $dksA_{Ct}$ promoter start site within *nrdR*. The number of detected matching sequences and genomic location within the *C. trachomatis* genome are indicated. The target site for the biotinylated oligonucleotide probe within $dksA_{Ct}$ is also shown. **(C)** A previously generated RNA-Seq data set (Grieshaber *et al.* 2018) was used to assess whether genes in the *nrdR-dksA-lspA* operon show temporal differences in expression ($n = 4$).

To independently verify the existence of two unique transcripts containing $dksA_{Ct}$, total RNA was extracted from *C. trachomatis*-infected HeLa cells at 20 and 30 hpi and northern blotting performed with oligonucleotide probes complementary to $dksA_{Ct}$. Blots indicate that $dksA_{Ct}$ is expressed as two transcripts with a prominent band at ~1.0 kb and a less prominent band at 1.5 kb (Fig. 7A). This pattern is consistent with polycistronic regulation via the 1.5 kb fragment, as the distance from the published TSS of *nrdR* to the *lspA* stop codon is 1477 bp (Albrecht *et al.* 2010). Characterization of the 1.0 kb fragment required additional verification due to the similar sizes of *nrdR* (465 bp) and *lspA* (504 bp). Therefore, we utilized neural network-based prediction software (Reese 2001) to search for sites within the identified operon region that may constitute an alternative promoter. Four sites were identified, one of which correlated directly with the TSS previously determined for *nrdR*. Of the other three predicted TSSs, two were located within *nrdR* and one within $dksA_{Ct}$. Using the predictions as a guide, 5′RACE was conducted using gene specific primers (GSPs) designed to bind within $dksA_{Ct}$ (Fig. 7B; Fig. S4, Supporting Information). Sequencing of 5′RACE fragments indicate a promoter site ~80–150 bp upstream of the $dksA_{Ct}$ ORF, which directly correlates with the 783880–783925 region predicted to contain the alternative promoter.

Transcript levels for $dksA_{Ct}$and the adjacent genes *nrdR* and *lspA* were determined by RNA-Seq at time points correlating with early, mid and late stages of the chlamydial developmental cycle (Fig. 7C). Data obtained by RNA-Seq support independent regulation of $dksA_{Ct}$ through a 5–6-fold increase in $dksA_{Ct}$ reads when compared with *nrdR*. Additionally, the expression pattern of $DksA_{Ct}$ (Fig. 1) correlates with the temporal pattern of transcript abundance observed in the RNA-Seq data set. As a final confirmation, quantitative reverse transcription polymerase chain reaction (RT-qPCR)-based transcriptional analysis conducted using cDNA extracted at 30 hpi indicated a 3–4-fold increase in $dksA_{Ct}$ transcript when compared with a region of *nrdR* upstream from the 5′RACE site (Fig. S5, Supporting Information). This increase

in transcript abundance corroborates data obtained by RNA-Seq, further supporting transcriptional regulation for $dksA_{Ct}$ from two independent promoters.

Conclusions

DksA has been described as one of eight transcription factors conserved across the phylum Chlamydiae (Domman and Horn 2015). Based upon data from previously studied C4-, C2- and C1-DksA orthologs, we predicted that $DksA_{Ct}$ is maintained as a protein associated with RB–EB transitions in the chlamydial developmental cycle. Herein, we showed that $DksA_{Ct}$ is expressed maximally at the RB–EB transition point (i.e. 15–20 hpi), a unique expression pattern compared with the stable expression observed for $DksA_{Ec}$ (Paul *et al.* 2004, Brown *et al.* 2002). Ectopic overexpression of $DksA_{Ct}$ prior to RB–EB transition produced a defect in both replication and EB generation. We found that $dksA_{Ct}$ does not functionally complement $dksA_{Ec}$ with respect to recovery of replication during growth on minimal medium. $DksA_{Ct}$has an overall domain structure similar to other C2- and C4-type DksA proteins despite containing only one cysteine residue. Upon comparing our C1-type DksA structure to the structure of other C2- and C4-type DksA proteins we speculate that the 'tip' of the coiled coil domain may be transiently structured/intrinsically disordered to assist binding to the secondary channel of RNAP. Expression of $DksA_{Ct}$ is likely regulated by tandem promoter regions, a regulatory scheme also described for other genes in this pathogen (Lambden *et al.* 1990, Rosario and Tan 2012). The phenotype resulting from induced $DksA_{Ct}$ expression prior to RB–EB transition and the correlation between $dksA_{Ct}$ and *nrdR* expression is consistent with a role for $DksA_{Ct}$ in the *C. trachomatis* developmental cycle. It should be mentioned that DksA can function in ways that could be beneficial to *C. trachomatis* even in the absence of a stringent response, including resolution of transcription conflicts (Tehranchi *et al.* 2010) and protection of phleomycin-induced double-stranded breaks in DNA (Sivaramakrishnan *et al.* 2017). Therefore, selective pressure to maintain *dksA* in chlamydiae could be related to such alternative functions.

It will be valuable to pursue loss of function phenotypes in future studies via deletion of $dksA_{Ct}$ (Mueller *et al.* 2017, Keb *et al.* 2018, Keb and Fields 2020) or CRISPR interference (Ouellette 2018, Ouellette *et al.* 2021) in case $dksA_{Ct}$ is essential to *C. trachomatis* intracellular replication and/or developmental transitions. Mechanistic understanding of how $DksA_{Ct}$ functions in *C. trachomatis* biology will require analysis of whether the protein directly influences pathogen gene expression by binding to RNAP akin to prototypical DksA proteins, or whether $DksA_{Ct}$ is associated with a different mechanism of action, such as interfering with the binding of another protein to RNAP, thus indirectly affecting transcriptional regulation.

Experimental procedures

Organisms and cell culture

Chlamydia trachomatis serovar L2 (LGV 434/Bu) was grown in the *Homo sapiens* cervix adenocarcinoma cell line HeLa or the murine fibroblast cell line McCoy (ATCC; Manassas, VA) cultured at 37°C with 5% CO_2 in RPMI 1640 (HyClone; Logan, UT) supplemented with 10% FetalPlex serum complex (Gemini; Sacramento, CA) and 10 μg/mL Gentamicin (MilliporeSigma; St Louis, MI).

Maintenance, purification and quantification of *Chlamydia*

Chlamydia trachomatis RB and EB cell forms were purified by density gradient centrifugation as previously described (Grieshaber *et al.* 2018). Chlamydial EBs were stored at −80°C in sucrose-phosphate-glutamate (Bovarnick *et al.* 1950) or K36 (Weiss 1965) buffer until use. Crude preparations of EBs for use in transformations were generated as previously described (Mueller *et al.* 2017). *Chlamydia trachomatis* was quantified by measurement of GE by SYBR green-based qPCR using a CFX96 or CFX384 real time PCR Detection System (BioRad, Hercules, CA) and primers targeting the *hctA* gene of *C. trachomatis*.

Plasmid construction and transformation of *C. trachomatis*

PCR primers used in this study are listed in Table S1 (Supporting Information). The vector pBOMB3cdMCI::*incD*-GFPLVA (Bauler and Hackstadt 2014) was linearized by PCR to remove the *incD* cassette using Q5 High-Fidelity DNA polymerase (New England Biolabs; Ipswich, MA). For *dksA* transcriptional fusion constructs, two inserts were generated spanning regions of 469 and 830 base pairs upstream from the annotated start site of *dksA*. For the E-Riboswitch *dksA* construct, *dksA* was inserted into pBOMB4 with an E-Riboswitch (Topp *et al.* 2010) driven by a T5 promoter to generate pBOMB4::E-Riboswitch-$dksA_{Ct}$. All DNA inserts were PCR-amplified using Phusion DNA polymerase (New England Biolabs; Ipswich, MA) and primer sets were generated according to the In-Fusion HD Cloning (Takara Bio, USA) guidelines. Linearized pBOMB4 and pBOMB4::GFPLVA were DpnI treated, then ligated to each insert and transformed into Stellar competent cells using the In-Fusion HD Cloning Kit (Takara Bio, USA). After incubation overnight at 37°C on LB agar plates containing 100 μg/mL carbenicillin (LB_{Carb}) (Chem-Impex International; Wood Dale, IL), colonies were selected for replating and screening via PCR. Plasmids were isolated using the Purelink Quick Plasmid Miniprep Kit (Invitrogen; Carlsbad, CA) and sequenced for insert confirmation. The confirmed plasmids were transformed into methyltransferase-deficient *E. coli* K-12 ER2925 competent cells and incubated overnight. Positive colonies were subcultured in 50 mL LB_{Carb} broth at 37°C, and unmethylated plasmids were isolated using the GenElute HP Endotoxin Free Plasmid Maxiprep Kit (MilliporeSigma; St Louis, MI). Eluted plasmids were either concentrated to ∼500 ng/μL using the DNA Clean and Concentrator-100 kit (Zymo Research; Irvine, CA) or via sodium acetate and isopropanol-mediated DNA precipitation. Unmethylated plasmids purified from *E. coli* were transformed into *C. trachomatis* essentially as described (Mueller *et al.* 2017). For some transformations of *C. trachomatis*, density gradient purified EBs (1×10^8 GE/well) were mixed with 2 μg of plasmid DNA. Cultures identified to have positive transformants as determined by fluorescence microscopy, were passaged two additional times to remove residual penicillin G susceptible bacteria and increase the titer of transformed cells. Clonal populations were generated via extraction of *C. trachomatis* from inclusions by micromanipulation repeated four times under limiting dilution. Plasmid DNA was obtained from isolated clones and transformed into *E. coli* where five colonies expressing mCherry were sequenced for confirmation of clonality.

Sequence analysis

Amino acid sequence alignments were done using the ClustalW (Thompson *et al.* 1994) alignment tool using MEGA software

(Tamura *et al.* 2021) and the MView multiple alignment viewer (Brown *et al.* 1998).

Escherichia coli complementation assay

Solid M9 medium was generated using Difco 5× M9 Minimal Salts, (Becton, Dickinson and Company; Franklin Lakes, NJ) supplemented with glycerol (0.4% v/v), $MgSO_4$ (2 mM), $CaCl_2$ (0.1 mM) and agar (1% w/v). Sterile filtered L-arabinose inducer was added at a final concentration of 0.1% (w/v) as indicated. *Escherichia coli* Δ*dksA* (strain: JW0141-1) was obtained from the Keio Knockout Collection, Yale University (Baba *et al.* 2006). $dksA_{Ec}$, $dksA_{Ct}$, $dksA1_{Pa}$ or $dksA2_{Pa}$ was ligated into the pBAD18 vector and transformed into *E. coli* Δ*dksA*. *Escherichia coli* K-12 was used as a positive control. Bacteria were plated and incubated for 24 h at 37°C, then imaged using a ChemiDoc Imaging System (Bio-Rad; Hercules, CA).

Analysis of $DksA_{Ct}$ expression

Protein lysates for analysis of $DksA_{Ct}$ expression by western blotting were obtained from 10–15 HeLa cell cultures (T-175) infected with *C. trachomatis* at an multiplicity of infection (MOI) of 300; bacteria were enriched by density gradient centrifugation using a 30% diatrizoate meglumine (MD-76R) pad essentially as described (Howard *et al.* 1974, Grieshaber *et al.* 2018). Bacteria were enumerated by analysis of GE, then lysed in Laemmli buffer containing β-mercaptoethanol (Bio-Rad; Hercules, CA) and heat denatured at 100°C for 10 min. Twelve % sodium dodecyl-sulfate polyacrylamide gel electrophoresis (SDS–PAGE) gels were loaded with the equivalent of 2×10^8 GE of each sample per well and electrophoresed at 25 mA for 40–60 min, then transferred to a 0.45 um PVDF membrane using a Trans-Blot Turbo transfer apparatus (Bio-Rad; Hercules, CA). The membrane was blocked in PBS + 0.1% Tween-20 (PBS-T) and 3% nonfat dry milk overnight at 4°C. The membrane was probed with a custom protein-A purified anti-$DksA_{Ct}$ antibody raised in rabbits against a truncated recombinantly expressed $DksA_{Ct}$ antigen in combination with a goat anti-rabbit poly-HRP secondary antibody (Invitrogen; Carlsbad, CA). The membrane was treated with the SuperSignal West Femto luminol and peroxide solution (ThermoFisher; Waltham, MA) and imaged using a ChemiDoc Imaging System (Bio-Rad; Hercules, CA). Animal use was approved by the Institutional Animal Care and Use Committee at Washington State University.

RNA extraction and northern blotting

HeLa cells were established in T-175 cell culture flasks and infected at an MOI of 300. At 20 and 30 hpi, cultures were disrupted by scraping in 1 mL K-36 buffer (Bovarnick *et al.* 1950) and centrifuged at 100 × *g* at 4°C for 3 min to remove large particles. Bacteria were pelleted from the supernatant via centrifugation at 20 000 × *g* at 4°C for 30 min. Pellets were then resuspended in 1 mL TRIzol reagent (Invitrogen, USA). HeLa RNA (control) was collected by scraping uninfected confluent monolayers in 4 mL TRIzol reagent. Samples were homogenized using a FastPrep 24 Tissue Homogenizer (MP Biomedicals; Santa Ana, CA) with 0.1 mm zirconia beads at 4 m/s for 20 s, repeated two times. Total RNA was extracted using chloroform, isopropanol and ethanol according to the manufacturer's protocol. RNA quantity was assessed using a Nanodrop Spectrophotometer (ThermoFisher; Waltham, MA), and RNA integrity measured using an Agilent 2100 Bioanalyzer (Agilent Technologies; Santa Clara, CA) and the RNA 6000 Nano Kit according to manufacturer's instructions.

Northern blotting of isolated total RNA was done using the NorthernMax Kit (Invitrogen, USA). PCR-generated *dksA* dsDNA was used as a positive control for detection. A custom 5′ Biotin tagged ssDNA oligonucleotide probe (Table S1, Supporting Information) was designed to bind *dksA* mRNA according to the ULTRAhyb Oligo Buffer (Invitrogen; Carlsbad, CA) recommendations. The RiboRuler high range RNA ladder and 2× loading dye (ThermoFisher; Waltham, MA) were used to assess mRNA size. The membrane was cut to match the exact size of the denaturing gel, and RNA transferred via capillary action for 2 h. The membrane was incubated in a UV crosslinker (Hoefer; Holliston, MA) for 1 min, repeated 3 times. The membrane was pre-hybridized with rotation in a 50 mL conical tube for 1 h in ULTRAhyb Oligo Buffer at 40°C. The probe was added to 3.5 mL buffer at a concentration of ∼600 pM and hybridized at 40°C for 17–20 h. The membrane was washed in the NorthernMax low stringency solution twice for 5 min at RT, and once at hybridization temperature for 2 min. The washed membrane was treated with the Chemiluminescence Nucleic Acid Detection Module Kit (ThermoFisher; Waltham, MA) according to the manufacturer's instructions, and imaged using a ChemiDoc Imaging System (Bio-Rad; Hercules, CA).

5′RACE

RNA isolated at 24 hpi was converted into cDNA tagged with the SMARTer II A Oligonucleotide using random hexamers as described in the SMARTer RACE 5′/3′ Kit (Takara Bio USA; Mountain View, CA). cDNA libraries were diluted as needed, and 5′RACE PCR reactions were run using three separate GSPs designed to target the intragenic $dksA_{Ct}$ sequence (Table S1, Supporting Information). PCR products were electrophoresed on a 1% TAE gel stained with SYBR Safe DNA Gel Stain (Invitrogen; Carlsbad, CA), and bands were excised for DNA isolation using the Nucleospin Gel and PCR Cleanup Kit (Macherey-Nagel; Düren, Germany). Fragments were then cloned using the CloneJET PCR cloning kit (ThermoFisher; Waltham, MA) and plasmids were isolated from positive transformants using the Nucleospin Plasmid Kit (Macherey-Nagel; Düren, Germany). Plasmids were sequencing using pJET1.2 vector specific primers (Eurofins Genomics). Clones were analyzed using NCBI BLAST against the *C. trachomatis* serovar L2 genome. Sequences not containing both the GSP and Universal Primer Mix regions, indicative of incomplete sequences, were excluded from the analysis.

PCR and RNA-Seq

cDNA for both conventional PCR analysis of polycistronic RNA and RT-qPCR applications was generated using the SuperScript III First-Strand Synthesis kit (Invitrogen; Carlsbad, CA) with RNA isolated at 20 and 30 hpi. Negative controls not containing reverse transcriptase were generated for each time point. Primers specific to *nrdR* and *lspA* (Table S1, Supporting Information) were utilized in conventional PCR to amplify cDNA for operon determination. For transcriptional analysis, *C. trachomatis* serovar L2 genomic DNA was extracted from density gradient purified EBs using phenol/chloroform precipitation. A dilution series of genomic DNA was generated and used for calculation of primer efficiencies and for calculation of relative copy number. Primer efficiencies between 85% and 110% were deemed acceptable for direct comparison of transcript levels. RNA-Seq data was recovered from a previously published data set (Grieshaber *et al.* 2018).

Ectopic expression of DksA in *C. trachomatis*

HeLa cells were grown to confluency in T-25 cell culture flasks. The culture medium was then replaced with RPMI-1640 supplemented with 10% (v/v) FetalPlex and 10 μg/mL Gentamicin. Each condition was tested in duplicate with two cultures supplemented with

0.5 mM theophylline and the other two serving as controls. Theophylline was added to the culture medium prior to inoculation. To facilitate comparative analysis, each flask was inoculated to reach equivalent levels (50–75%) of infection using bacteria carrying the pBOMB4::E-Riboswitch-*dksA*$_{Ct}$ or p2TK2-SW2::E-Riboswitch-Clover (Grieshaber *et al*, 2022) vectors and incubated at 37°C in a 5% CO_2 incubator for 30 h. Induction of pBOMB4::E-Riboswitch-*dksA*$_{Ct}$ results in expression of an untagged DksA$_{Ct}$ protein. The medium was then removed, and HeLa cell monolayers were washed with K-36 buffer. Infected host cells were disrupted by vigorous scraping in K-36 buffer and then host cell debris was removed from the mixture via centrifugation at 100 × *g* for 3 min at 4°C. The supernatant was removed, and *Chlamydia* was pelleted at 20 000 × *g* for 15 min at 4°C. Pelleted bacteria were resuspended in 30 μL SPG and frozen at −80°C. GEs were enumerated using qPCR and IFU assays were conducted using HeLa cells grown to confluency in 12-well plates with inocula normalized to GE.

Microscopy

Micrographs were acquired using a Leica DMi8 inverted microscope (Leica Microsystems; Buffalo Grove, IL) equipped with an X-Cite LED light source and DMC2900 camera. *Chlamydia trachomatis* IFU assays were done using methanol fixed samples stained with a fluorescein isothiocyanate-tagged anti-MOMP antibody (PA1-73073 Thermo Fisher; Waltham, MA) at 1/250 dilution in PBS buffer. Images were analyzed and processed using ImageJ (The National Institute of Health; Bethesda, MD). Adjustments of contrast or signal intensity were applied to the entire image.

Cloning of *dksA*$_{Ct}$

The *dksA*$_{Ct}$ gene (Gene ID: 5858340) was amplified from the genomic DNA of *C. trachomatis* serovar L2 (LGV 434/Bu) (NCBI: 471472) and inserted into the expression vector BG1861 (a derivative of pET14b) (Myler *et al.* 2009) at a site containing an uncleavable, 8-residue N-terminal tag (MAHHHHHH-). Using a heat shock method, the recombinant plasmid was used to transform *E. coli* BL21(DE3)-R3-pRARE2 cells (gift from SGC Toronto). From these transformed cells, stocks were prepared (∼1 mL LB media, OD_{600} ∼0.8) from a single colony and stored at −80°C in glycerol (∼15%) solution until preparation of samples for structural analysis.

Crystallization, X-ray data collection and structure refinement of DksA$_{Ct}$

For X-ray crystallographic analysis, DksA$_{Ct}$ was expressed and purified following standard SSGCID protocols (Bryan *et al.* 2011). The protein was concentrated to 24.6 mg/mL in 25 mM HEPES, 500 mM NaCl, 5% (v/v) glycerol, 2 mM DTT, and 0.025% sodium azide (v/v), pH 7.5. Initial crystallization conditions were searched for using 0.4 (protein) plus 0.4 (precipitant) μL drops in XJR crystallization trays (Rigaku Reagents; Bainbridge Island, WA) and several commercial screens: JCSG+, JCSG-Top96, Wizard 1/2, Wizard 3/4 (Rigaku Reagents; Bainbridge Island, WA), Crystal Screen, IndexHR (Hampton Research; Aliso Viego, CA), MCSG-1, MCSG-2 (Microlytic/Anatrace; Maumee, OH), Morpheus 1 and 2, PACT (Molecular Dimensions; Holland, OH). Initial crystal hits were optimized starting from CrystalScreen, condition B5: 200 mM lithium sulfate, 25% (w/v) PEG 4000, 100 mM Tris, pH 8.5. The crystals were cryoprotected with 15% ethylene glycol and vitrified in nylon loops by plunging into liquid nitrogen. Diffraction data up to 2.95 Å resolution were collected at the Advanced Photon Source (APS), Live Sciences Collaborate Access Team (LS-CAT) beamline 21-ID-F, at a wavelength of 0.97872 Å with a Rayonix MX-300 detector. Diffraction data statistics are summarized in Table 1. The structure could not be solved using the standard SSGCID molecular replacement strategies. However, with MR-Rosetta (Terwilliger *et al.* 2012) as implemented in Phenix (Adams *et al.* 2011), a dimer solution could be found that was based on PDB entries 4IJJ_A, 1TJL_H, 2KQ9_A, 2KGO_A and 5W1S_N. The structure was then completed with iterative refinement cycles in phenix.refine (Zwart *et al.* 2008), and real space modeling in Coot (Emsley *et al.* 2010). The quality of the model was assessed with tools built into Coot and phenix.refine, such as MolProbity (Williams *et al.* 2018). The coordinates and structure factors were deposited in the PDB with code 6PTG. Diffraction images are available at proteindiffraction.org.

Statistical analysis

Statistical analyses were conducted using Prism (GraphPad Inc.; San Diego, CA) software. Statistical analysis and normalization of read counts for RNA-Seq data (Fig. 7) was done using DESeq2 in R (Love *et al.* 2014). Normalization from Dseq2 was used for transcript visualization in Integrated Genomics Viewer (Robinson *et al.* 2011).

Acknowledgments

Plasmids pBOMB3cdMCI::*incD*-GFPLVA and pBOMB4::tet-mCherry were generous gifts from Ted Hackstadt (Rocky Mountain Laboratories, NIAID, NIH). We thank John-Demian Sauer, University of Wisconsin, Madison, for the inducible riboswitch E.

Funding

This work was supported by a New Faculty Seed Grant and laboratory start-up funds from Washington State University, R21AI115244 (AO) and R01AI130072 (AO, SG). Structural analysis of DksA$_{Ct}$ was supported by the Seattle Structural Genomics Center for Infectious Disease (SSGCID), which is funded by the National Institute of Allergy and Infectious Diseases, National Institutes of Health, Department of Health and Human Services under Federal Contract number HHSN272201700059C. The SSGCID internal ID for DksA$_{Ct}$ is ChtrB.19237.a.B1 (www.ssgcid.org). CM was supported by a T-32 training grant, 5T32AI007025-39 (T. H. Kawula). Part of the research was conducted at the W.R. Wiley Environmental Molecular Sciences Laboratory, a national scientific user facility sponsored by the U.S. Department of Energy's Office of Biological and Environmental Research (BER) program located at Pacific Northwest National Laboratory (PNNL). Battelle operates PNNL for the U.S. Department of Energy. This research also used resources of the Advanced Photon Source, a U.S. Department of Energy (DOE) Office of Science User Facility operated for the DOE Office of Science by Argonne National Laboratory under Contract No. DE-AC02-06CH11357. Use of the LS-CAT Sector 21 was supported by the Michigan Economic Development Corporation and the Michigan Technology Tri-Corridor (Grant 085P1000817).

The content is solely the responsibility of the authors and does not necessarily represent the official views of the National Institutes of Health.

Supplementary data

Supplementary data are available at *FEMSPD* online.

Contributions

CM, HY, GWB, JA, TC, NG, SG and AO designed and performed experiments and analyzed data. CM and AO wrote the manuscript.

CM, HY, GWB, JA, TC, NG, SG and AO edited the manuscript. AO designed the study.

Data availability

The data underlying this article are available via Protein Data Bank and proteindiffraction.org and can be accessed with PDB identifier 6PTG.

Conflict of interest statement. The authors have no conflicts of interest to declare.

References

Adams PD, Afonine PV, Bunkóczi G *et al.* The Phenix software for automated determination of macromolecular structures. *Methods* 2011;**55**:94–106.

Albrecht M, Sharma CM, Dittrich MT *et al.* The transcriptional landscape of *Chlamydia pneumoniae*. *Genome Biol* 2011;**12**:R98.

Albrecht M, Sharma CM, Reinhardt R *et al.* Deep sequencing-based discovery of the *Chlamydia trachomatis* transcriptome. *Nucleic Acids Res* 2010;**38**:868–77.

Baba T, Ara T, Hasegawa M *et al.* Construction of *Escherichia coli* K-12 in-frame, single-gene knockout mutants: the Keio collection. *Mol Syst Biol* 2006;**2**:2006.0008.

Bauler LD, Hackstadt T. Expression and targeting of secreted proteins from *Chlamydia trachomatis*. *J Bacteriol* 2014;**196**:1325–34.

Belland RJ, Zhong G, Crane DD *et al.* Genomic transcriptional profiling of the developmental cycle of *Chlamydia trachomatis*. *Proc Natl Acad Sci USA* 2003;**100**:8478–83.

Blaby-Haas CE, Furman R, Rodionov DA *et al.* Role of a Zn-independent DksA in Zn homeostasis and stringent response. *Mol Microbiol* 2011;**79**:700–15.

Bovarnick MR, Miller JC, Snyder JC. The influence of certain salts, amino acids, sugars, and proteins on the stability of rickettsiae. *J Bacteriol* 1950;**59**:509–22.

Brothwell JA, Muramatsu MK, Toh E *et al.* Interrogating genes that mediate *Chlamydia trachomatis* survival in cell culture using conditional mutants and recombination. *J Bacteriol* 2016;**198**:2131–9.

Brown L, Gentry D, Elliott T *et al.* DksA Affects ppGpp Induction of RpoS at a Translational Level. *J Bacteriol* 2002;**184**:4455–4465.

Brown NP, Leroy C, Sander C. MView: a web-compatible database search or multiple alignment viewer. *Bioinformatics* 1998;**14**:380–1.

Bryan CM, Bhandari J, Napuli AJ *et al.* High-throughput protein production and purification at the Seattle Structural Genomics Center for Infectious Disease. *Acta Crystallogr Sect F Struct Biol Cryst Commun* 2011;**67**:1010–4.

Burton MJ, Mabey DCW. The global burden of trachoma: a review. *PLoS Negl Trop Dis* 2009;**3**:e460.

Capra JA, Singh M. Predicting functionally important residues from sequence conservation. *Bioinformatics* 2007;**23**:1875–82.

Cashel M, Gallant J. Two compounds implicated in the function of the RC gene of *Escherichia coli*. *Nature* 1969;**221**:838–41.

Cashel M, Gentry DR, Hernandez VJ *et al.* The stringent response. In: *Escherichia coli and Salmonella Cellular and Molecular Biology*. Vol. **2**. Washington, DC: ASM Press, 1996.

Clark K, Karsch-Mizrachi I, Lipman DJ *et al.* GenBank. *Nucleic Acids Res* 2016;**44**:D67–72.

Crawford MA, Tapscott T, Fitzsimmons LF *et al.* Redox-active sensing by bacterial DksA transcription factors is determined by cysteine and zinc content. *mBio* 2016;**7**:e02161–15.

Dalebroux ZD, Yagi BF, Sahr T *et al.* Distinct roles of ppGpp and DksA in *Legionella pneumophila* differentiation. *Mol Microbiol* 2010;**76**:200–19.

Domman D, Horn M. Following the footsteps of chlamydial gene regulation. *Mol Biol Evol* 2015:msv193.

Emsley P, Lohkamp B, Scott WG *et al.* Features and development of Coot. *Acta Crystallogr D Biol Crystallogr* 2010;**66**:486–501.

Erdős G, Dosztányi Z. Analyzing protein disorder with IUPred2A. *Curr Protoc Bioinformatics* 2020;**70**:e99.

Ferullo DJ, Lovett ST. The stringent response and cell cycle arrest in *Escherichia coli*. *PLoS Genet* 2008;**4**:e1000300.

Furman R, Biswas T, Danhart EM *et al.* DksA2, a zinc-independent structural analog of the transcription factor dksA. *FEBS Lett* 2013;**587**:614–9.

Garner E, Romero P, Dunker AK *et al.* Predicting binding regions within disordered proteins. *Genome Inform* 1999;**10**:41–50.

Geiger T, Goerke C, Fritz M *et al.* Role of the (p)ppGpp synthase RSH, a RelA/SpoT homolog, in stringent response and virulence of *Staphylococcus aureus*. *Infect Immun* 2010;**78**:1873–83.

Grieshaber N, Chiarelli TJ, Appa CR *et al.* Translational gene expression control in *Chlamydia trachomatis*. *Plos One* 2022;**17**:e0257259.

Grieshaber S, Grieshaber N, Yang H *et al.* Impact of active metabolism on *Chlamydia trachomatis* elementary body transcript profile and infectivity. *J Bacteriol* 2018;**200**:e00065–18.

Hauryliuk V, Atkinson GC, Murakami KS *et al.* Recent functional insights into the role of (p)ppGpp in bacterial physiology. *Nat Rev Microbiol* 2015;**13**:298–309.

Henard CA, Tapscott T, Crawford MA *et al.* The 4-cysteine zinc-finger motif of the RNA polymerase regulator DksA serves as a thiol switch for sensing oxidative and nitrosative stress. *Mol Microbiol* 2014;**91**:790–804.

Howard L, Orenstein NS, King NW. Purification on renografin density gradients of *Chlamydia trachomatis* grown in the yolk sac of eggs. *Appl Microbiol* 1974;**27**:102–6.

Jude F, Köhler T, Branny P *et al.* Posttranscriptional control of quorum-sensing-dependent virulence genes by DksA in *P seudomonas aeruginosa*. *J Bacteriol* 2003;**185**:3558–66.

Keb G, Fields KA. Markerless gene deletion by floxed cassette allelic exchange mutagenesis in *Chlamydia trachomatis*. *J Vis Exp* 2020;**155**:e60848. DOI: 10.3791/60848.

Keb G, Hayman R, Fields KA. Floxed-cassette allelic exchange mutagenesis enables marker-less gene deletion in *Ch lamydia trachomatis* and can reverse cassette-induced polar effects. *J Bacteriol* 2018;**200**:e00479–18.

Kessler JR, Cobe BL, Richards GR. Stringent response regulators contribute to recovery from glucose phosphate stress in *Escherichia coli*. *Appl Environ Microbiol* 2017;**83**:e01636–17.

Konrat R. NMR contributions to structural dynamics studies of intrinsically disordered proteins. *J Magn Reson* 2014;**241**:74–85.

Krissinel E. On the relationship between sequence and structure similarities in proteomics. *Bioinformatics* 2007;**23**:717–23.

Lambden PR, Everson JS, Ward ME *et al.* Sulfur-rich proteins of *Chlamydia trachomatis*: developmentally regulated transcription of polycistronic mRNA from tandem promoters. *Gene* 1990;**87**:105–12.

Lennon CW, Lemmer KC, Irons JL *et al.* A *Rhodobacter sphaeroides* protein mechanistically similar to *Escherichia coli* DksA regulates photosynthetic growth. *mBio* 2014;**5**:e01105–14.

Lennon CW, Ross W, Martin-Tumasz S *et al.* Direct interactions between the coiled-coil tip of DksA and the trigger loop of RNA polymerase mediate transcriptional regulation. *Genes Dev* 2012;**26**:2634–46.

Love MI, Huber W, Anders S. Moderated estimation of fold change and dispersion for RNA-seq data with DESeq2. *Genome Biol* 2014;**15**:550.

Magnusson LU, Farewell A, Nyström T. ppGpp: a global regulator in *Escherichia coli*. *Trends Microbiol* 2005;**13**:236–42.

Magnusson LU, Gummesson B, Joksimovic P *et al.* Identical, independent, and opposing roles of ppGpp and DksA in *Escherichia coli*. *J Bacteriol* 2007;**189**:5193–202.

Mészáros B, Erdős G, Dosztányi Z. IUPred2A: context-dependent prediction of protein disorder as a function of redox state and protein binding. *Nucleic Acids Res* 2018;**46**:W329–37.

Mittenhuber G. Comparative genomics and evolution of genes encoding bacterial (p)ppGpp synthetases/hydrolases (the rel, RelA and SpoT proteins). *J Mol Microbiol Biotechnol* 2001;**3**:585–600.

Molodtsov V, Sineva E, Zhang L *et al.* Allosteric effector ppGpp potentiates the inhibition of transcript initiation by dksA. *Mol Cell* 2018;**69**:828–39.

Mueller KE, Wolf K, Fields KA. *Chlamydia trachomatis* transformation and allelic exchange mutagenesis: *Chlamydia trachomatis* transformation and mutagenesis. In: Coico R, McBride A, Quarles JM *et al.* (eds). *Current Protocols in Microbiology*. Hoboken, NJ: John Wiley & Sons, Inc., 2017, 11A.3.1–15.

Mukhopadhyay S, Good D, Miller RD *et al.* Identification of *Chlamydia pneumoniae* proteins in the transition from reticulate to elementary body formation. *Mol Cell Proteomics* 2006;**5**:2311–8.

Myler P, Stacy R, Stewart L *et al.* The Seattle Structural Genomics Center for Infectious Disease (SSGCID). *Infect Disord Drug Targets* 2009;**9**:493–506.

Oldfield CJ, Xue B, Van Y-Y *et al.* Utilization of protein intrinsic disorder knowledge in structural proteomics. *Biochim Biophys Acta* 2013;**1834**:487–98.

Omsland A, Sager J, Nair V *et al.* Developmental stage-specific metabolic and transcriptional activity of *Chlamydia trachomatis* in an axenic medium. *Proc Natl Acad Sci USA* 2012;**109**:19781–5.

Ouellette SP, Blay EA, Hatch ND *et al.* CRISPR interference to inducibly repress gene expression in *Chlamydia trachomatis*. *Infect Immun* 2021;**89**:e0010821.

Ouellette SP. Feasibility of a conditional knockout system for *Chlamydia* based on CRISPR interference. *Front Cell Infect Microbiol* 2018;**8**:59.

Pal RR, Bag S, Dasgupta S *et al.* Functional characterization of the stringent response regulatory gene *dksA* of *Vibrio cholerae* and its role in modulation of virulence phenotypes. *J Bacteriol* 2012;**194**:5638–48.

Parshin A, Shiver AL, Lee J *et al.* DksA regulates RNA polymerase in *Escherichia coli* through a network of interactions in the secondary channel that includes sequence insertion 1. *Proc Natl Acad Sci USA* 2015;**112**:E6862–71.

Paul BJ, Barker MM, Ross W *et al.* DksA: a critical component of the transcription initiation machinery that potentiates the regulation of rRNA promoters by ppGpp and the initiating NTP. *Cell* 2004;**118**:311–22.

Paul BJ, Berkmen MB, Gourse RL. DksA potentiates direct activation of amino acid promoters by ppGpp. *Proc Natl Acad Sci USA* 2005;**102**:7823–8.

Perederina A, Svetlov V, Vassylyeva MN *et al.* Regulation through the secondary channel–structural framework for ppGpp–DksA synergism during transcription. *Cell* 2004;**118**:297–309.

Perron K, Comte R, Van Delden C. DksA represses ribosomal gene transcription in *Pseudomonas aeruginosa* by interacting with RNA polymerase on ribosomal promoters. *Mol Microbiol* 2005;**56**:1087–102.

Potrykus K, Cashel M. (p)ppGpp: still magical? *Annu Rev Microbiol* 2008;**62**:35–51.

Reese MG. Application of a time-delay neural network to promoter annotation in the *Drosophila melanogaster* genome. *Comput Chem* 2001;**26**:51–6.

Robinson JT, Thorvaldsdóttir H, Winckler W *et al.* Integrative genomics viewer. *Nat Biotechnol* 2011;**29**:24–6.

Rosario CJ, Tan M. The early gene product EUO is a transcriptional repressor that selectively regulates promoters of *Chlamydia* late genes. *Mol Microbiol* 2012;**84**:1097–107.

Rowley J, Toskin I, Ndowa F *et al. Global Incidence and Prevalence of Selected Curable Sexually Transmitted Infections, 2008*. Geneva, Switzerland: World Health Organization, 2012.

Rutherford ST, Lemke JJ, Vrentas CE *et al.* Effects of DksA, GreA, and GreB on transcription initiation: insights into the mechanisms of factors that bind in the secondary channel of RNA polymerase. *J Mol Biol* 2007;**366**:1243–57.

Shaw EI, Dooley CA, Fischer ER *et al.* Three temporal classes of gene expression during the *Chlamydia trachomatis* developmental cycle. *Mol Microbiol* 2000;**37**:913–25.

Sivaramakrishnan P, Sepúlveda LA, Halliday JA *et al.* The transcription fidelity factor GreA impedes DNA break repair. *Nature* 2017;**550**:214–8.

Skipp PJS, Hughes C, McKenna T *et al.* Quantitative proteomics of the infectious and replicative forms of *Chlamydia trachomatis*. *PLoS One* 2016;**11**:e0149011.

Stamm WE. *Chlamydia trachomatis* infections: progress and problems. *J Infect Dis* 1999;**179**:S380–3.

Stephens RS. Genome sequence of an obligate intracellular pathogen of humans: *Chlamydia trachomatis*. *Science* 1998;**282**:754–9.

Tamura K, Stecher G, Kumar S. MEGA11: molecular evolutionary genetics analysis version 11. *Mol Biol Evol* 2021;**38**:3022–7.

Tehranchi AK, Blankschien MD, Zhang Y *et al.* The transcription factor DksA prevents disruption of DNA replication upon nutritional stress. *Cell* 2010;**141**:595–605.

Terwilliger TC, DiMaio F, Read RJ *et al.* phenix.mr_rosetta: molecular replacement and model rebuilding with Phenix and Rosetta. *J Struct Funct Genomics* 2012;**13**:81–90.

Thompson JD, Higgins DG, Gibson TJ. CLUSTAL W: improving the sensitivity of progressive multiple sequence alignment through sequence weighting, position-specific gap penalties and weight matrix choice. *Nucleic Acids Res* 1994;**22**:4673–80.

Tian W, Skolnick J. How well is enzyme function conserved as a function of pairwise sequence identity? *J Mol Biol* 2003;**333**:863–82.

Topp S, Reynoso CMK, Seeliger JC *et al.* Synthetic riboswitches that induce gene expression in diverse bacterial species. *Appl Environ Microbiol* 2010;**76**:7881–4.

Traxler MF, Summers SM, Nguyen H-T *et al.* The global, ppGpp-mediated stringent response to amino acid starvation in *Escherichia coli*. *Mol Microbiol* 2008;**68**:1128–48.

Vinella D, Potrykus K, Murphy H *et al.* Effects on growth by changes of the balance between GreA, GreB, and DksA suggest mutual competition and functional redundancy in *Escherichia coli*. *J Bacteriol* 2012;**194**:261–73.

Weiss E. Adenosine triphosphate and other requirements for the utilization of glucose by agents of the psittacosis-trachoma group. *J Bacteriol* 1965;**90**:243–53.

Williams CJ, Headd JJ, Moriarty NW *et al.* MolProbity: more and better reference data for improved all-atom structure validation. *Protein Sci* 2018;**27**:293–315.

Zwart PH, Afonine PV, Grosse-Kunstleve RW *et al.* Automated structure solution with the PHENIX suite. *Methods Mol Biol* 2008;**426**:419–35.